

Experimental and Simulation Analysis on Stress Developed , Deformation and Modes of Failure of Cables and Beam in Post Tensioning Process

Rabin Hamal ^a, Sunil Adhikari ^b

^{a, b} Department of Automobile and Mechanical Engineering, Thapathali Campus, IOE, Tribhuvan University, Nepal

Corresponding Email: ^a maindus069@gmail.com

Abstract

The use of prestressing in different structures has increased tremendously where the tensile force of the cable is used to provide the compressive force to the concrete. In the present context of Nepal, mainly post-tensioning process is used as the prestressing method in which the stress in cable attains pre-stress at the anchorage block after the maturity of the concrete. The objectives of this study are to find the ultimate tensile strength of the cable, deflection of the beam, and causes of failure of the cable and beam during the post-tensioning process. A mathematical and 3D finite element modeling of post-tensioned concrete beam were used to study the effects of the cable profile, eccentricity, and the magnitude of prestressing force. The deflection of the beam varied significantly on different cable profiles, eccentricity, and pre-stressing force on the cable. The maximum upward deflection was found on the beam with parabolic profile beam, the deflection rises with the increase in the eccentricity and the pre-stressing force. The accuracy of the results obtained from the ANSYS model was validated by comparing it with the result of the mathematical model.

Keywords

Pre-stressing, Pre-tensioning, Post-tensioning, anchorage block, 3D finite element, cable profile, eccentricity

1. Introduction

During the past half-century, the use of pre-stressing in different structures has increased tremendously. It is most frequently used as a key method in the construction of bridges, parking structures, buildings, slabs, railway sleepers, transmission poles, etc. Pre-stressing is the method of inducing known permanent stresses in the structure or member before the full-service load is applied. It is known that the concrete is weak in tension and strong in compression. In pre-stressing the tensile force in the cable is used to provide a compressive force to the concrete.

Pre-stressing in structures can be done by two different processes namely: pre-tensioning and post-tensioning. In pre-tensioning the force is provided to the cable with the reaction against rigid support before the casting of the concrete whereas, in the post-tensioning process, the ducts of the cable or strands are placed along with the reinforcement before casting of the concrete. The cables are stressed from a single end or both ends with the reaction acting against the matured concrete.

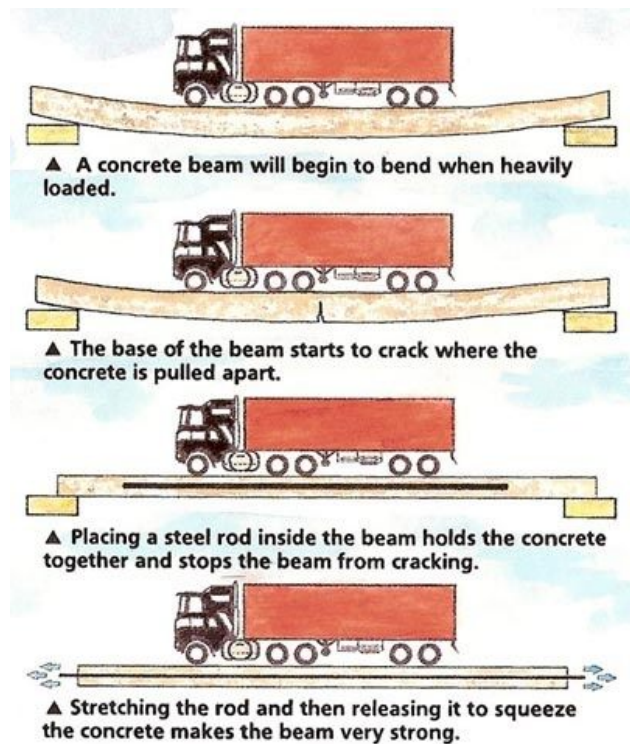


Figure 1: Effect of pre stressing [1]

2. Methodology

2.1 Literature Review

Various studies have been carried out to find the deflection and stress concentration of the post-tensioned beam during the post-tensioning process. The prestressing forces counteract the downward deflection caused due to the dead load and live load. The numerical methods has been used to find the deflection due to the prestressing force, the dead load of the beam and the live load acted upon the beam. Also, the finite element method is used to validate the values of the numerical method. The post-tensioned beam has fewer rebars than the RCC beam. The load of the beam is supported by the pre-stress cables anchored at the end of the beams. So the stress concentration is higher at the anchorage which can result in the failure of anchorage and the concrete at that region. Also, concrete beam failure occurs at regions where tensile and compressive stresses are higher.

Aimee Corn in "Failure mode analysis of Post-tension anchored dam" used linear finite element analysis to study the tensile and shear failure of the concrete dam. The results from the study y indicate demand to capacity ratios (DCR) of 0.79 for the anchor head, 0.75 for the tendon, and 0.63 for the foundation cone failure, and a potential displacement of 0.33 inches, which is not large enough to shear the tendon [2].

Ah Sir Cho in "Load-Carrying Performance and Hydrostatic Tests of Encapsulated Anchor Systems for Unbonded Post-Tensioning Single-Strands" conducted the various tests to The use encapsulation system for unbounded single-strand tendon for the purpose of corrosion protection and enhanced durability. In the study, load-carrying performance and hydrostatic tests of the developed encapsulation anchor were undertaken according to the Korean and U.S. testing standards. Static load and fatigue tests were used to evaluate the load-carrying performance of the tendon assembly and mechanical interactions between the wedge and strand or anchor. The stable behavior was verified under static load and cyclic load. The anchor slip was only approximately 3 mm, which was about half the typical wedge slip of 6 to 9 mm. The fracture of the strand occurred at 4% elongation, which is considered to be quite large. The waterproofness of the encapsulation system was confirmed via a hydrostatic test.

Kim, J.H. Choi in "Nonlinear finite element analysis of

unbonded post-tensioned concrete beams" developed a sophisticated 3-D finite element model formulating the non linear flexural behavior of unbonded post-tensioned beams to compare analysis results with experimental results to varyify the accuracy of the developed 3-D finite element model and to investigate the effects of various prestressing forces on the flexural behavior of post-tensioned beam. From the comparison results, a modification factor of 0.75 was recommended to predict the load deflection behavior of unbonded post-tensioned beas using the proposed ANSYS model in the study conservatively.

Kevin Q. Walsh in "Effects of loading conditions on the behavior of unbonded post-tensioning strand-anchorage systems" investigated the strand fracture strains of unbonded post-tensioning strand-anchorage systems under different loading conditions. In addition, stress-strain relationships were proposed for seven-wire, low-relaxation, uncoated 270 ksi (1860 MPa) prestressing strand. The research presented an experimental investigation on the strand wire fracture stresses and strains in unbonded post-tensioning strand-anchorage systems subjected to a variety of loading conditions that can affect the performance of the strand inside the anchor. While unbonded post-tensioned gravity load systems are common throughout the United States, the use of this construction technique for the seismic-resistant structures can put the strands under significantly greater strain demands. Strand wire fractures can occur inside the anchorages, limiting the seismic performnce of the structure [3].

The use of experimental data of the cable for the simulation and analytical method can provide more realistic results. So the experimental test data of the cable and beam is used in simulation and analytical method to study the effects of prestressing forces, cable profile, and eccentricity on the stresses and deformation of the beam.

2.2 Testing of systems with mechanical anchorages

The static load test helps to assess the performance of the cable-anchorage assembly. All components necessary for anchoring the cable should be included in the cable anchorage assembly to be tested, as determined by its intended application. Testing is performed on the cable specimen by mounting it in a testing machine or ring, and stressing it at one end with equipment similar to that used on a construction

site. In steps corresponding to 0.1, 0.2, 0.3, 0.4. . . . 1 percent extension of the strand and corresponding load is studied[3]. Breaking load of the strand shall be recorded and mode of failure is studied.



Figure 2: Setup for static load test

The relaxation test with tendon anchorage assembly is used to find out the relaxation loss of the cable over the specified period of time. 70 percent of the breaking load is applied to the pre-stress strand and is allowed to relax in a closed chamber machine and the loss in the stress is studied over the time of 100 hrs.



Figure 3: Setup for Relaxation test

A jacking test is a simple experiment that simulates the post-tensioning process by measuring the jacking force by means of a load cell installed between the live-end anchor and the jack. This setup is similar to that used in precast plants. Single pull jack is used to stress a single strand where the other side is anchored. The slip in the strand and wedge assembly is studied at one end during the process where it is stressed from the other ends of the beam. Push-in tests will be carried out to test the strength of an anchor when a three-piece wedge is pushed in, both with and without an offset

or gap between the pieces[4].The breaking load of the cable will be calculated using jacking force and slipping of the cable at anchorage will be studied with simultaneous increase in the jacking force.

2.3 Mathematical Equation and Calculation

Here a post-tensioned beam is modelled in ANSYS for the analysis of the stress developed at various regions, the effect of the cable profile on the load applied on the beam, the deflections on the beam due to post-tensioning, and loads applied on the beam. Also the effect of the amount of prestressing forces and the losses due to various phenomenon. The beam is modelled the same as that discussed in the paper "Nonlinear Finite Element Analysis of Unbonded Post Tensioned Concrete Beam" [5]. In the mathematical model, the deflection due to prestressing force is calculated by the load-balancing method.

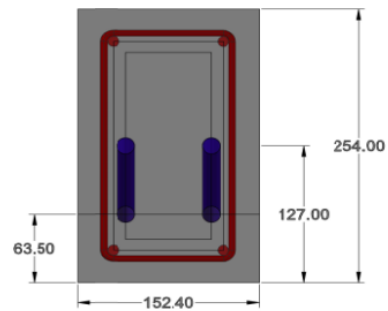


Figure 4: Section view of beam

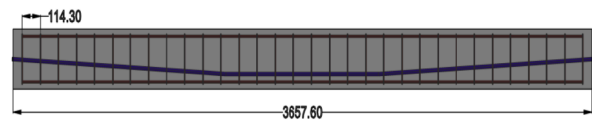


Figure 5: Side view of beam

Parabolic Profile Beam For post-tensioned beam analysis, concrete and cable are both to be studied individually. For parabolic profiles, pre-stress force from the cable is converted to equivalent uniformly distributed load. At first the bending moment diagram is drawn for the parabolic profile which is given by the equation of parabola.

$$y = Ax^2 + Bx + C \tag{1}$$

Differentiating equation (1) we get,

$$\frac{dy}{dx} = 2Ax + B \tag{2}$$

Again differentiating equation (2) we get,

$$\frac{d^2y}{dx^2} = 2A(\text{constant}) \quad (3)$$

From this we know that the load that gives shear force and bending moment is a constant load. From the bending moment diagram we can say that the maximum moment occurs at the center where the value of eccentricity is maximum, Let a be the maximum eccentricity i.e. $e_{max} = a$

Moment = Force in tendon * eccentricity at center

$$M = F * a \quad (4)$$

Also the integral of shear force diagram = Moment

$$= \left(\frac{1}{2} * \frac{L}{2} * W \frac{L}{2}\right) = W \frac{L^2}{8} \quad (5)$$

Equating equation(4) and (5), we get

$$W \frac{L^2}{8} = F * a \quad (6)$$

Hence equation (6) gives the value of equivalent uniformly distributed load on beam due to the prestress force on the cable.

$$W = \frac{8F * a}{L^2} \quad (7)$$

The maximum deflection due to the equivalent uniformly distributed load is given by the equation:

$$\Delta_{max} = \frac{5 * W * L^4}{384 * E * I} \quad (8)$$

Where, W is the equivalent load, L is the span length, E is the modulus of elasticity of concrete and I is moment of inertia of the beam.

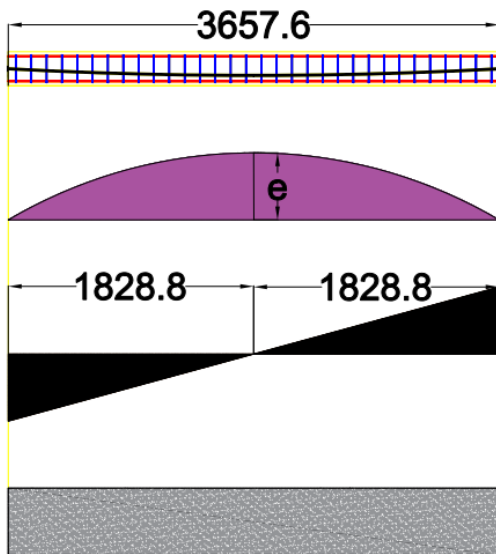


Figure 6: SFD, BMD and ELD for Parabolic profile beam

Trapezoidal Profile Beam For the trapezoidal profile, the force on the cable is converted into equivalent two equal point loads. The two equal point loads acting at equal distance from two ends are given by the vertical component of the force on the cable. The vertical point loads due to the prestressing force give the upward deflection which is maximum at the center of the beam.

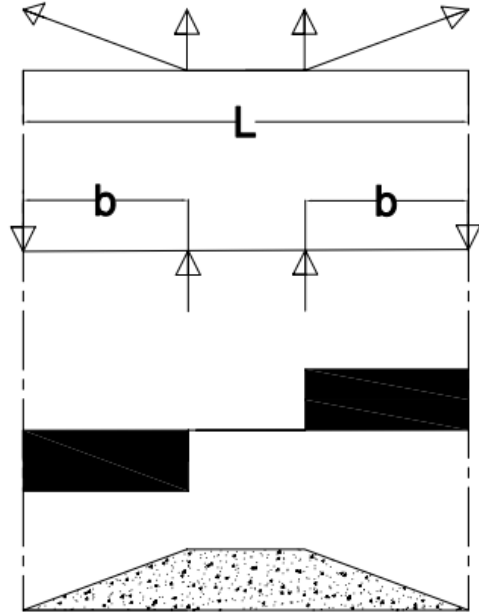


Figure 7: SFD, BMD and ELD for Trapezoidal profile beam

$$P = F \sin \theta \quad (9)$$

Where F is prestress force on the cable.

$$P_1 = P_2 = P = F \frac{a}{b} \quad (10)$$

Maximum deflection of the beam due to two point loads is given by the equation:

$$\Delta_{max} = \frac{P * b * (3 * L^2 - 4 * b^2)}{24 * E * I} \quad (11)$$

Sloping profile Beam For the sloping tendon, the equivalent load is simply a point load which is the vertical component of the force on the cable. From the bending moment diagram, maximum bending moment is at the center.

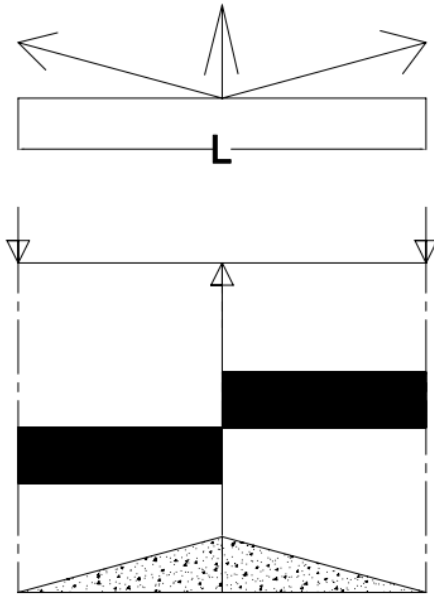


Figure 8: SFD,BMD and ELD for Slopping profile beam

$$M_{max} = \frac{P}{2} * \frac{L}{2} \quad (12)$$

Where P is the equivalent point load and L is the length of the span. Also, we know the maximum bending moment is equal to multiplication of force on the cable and eccentricity.

$$M_{max} = F * a \quad (13)$$

Equating equation (12) and (13) we get;

$$\frac{P * L}{4} = F * a \quad (14)$$

$$P = \frac{4 * F * a}{L} \quad (15)$$

And the maximum deflection due to point load is given by the formula;

$$\Delta_{max} = \frac{P * L^3}{48 * E * I} \quad (16)$$

2.4 Finite Element Model

ANSYS software was used for finite element modeling and analysis. ANSYS software is easily the most popular and reliable finite element method program available. For the geometry needed for the

simulation, a 3D model is required. It was easier to build a 3D model in other 3D drafting software. AUTOCAD2015 was used to make a 3D geometry, a rectangular section of width 152.4 mm and depth 254 mm was made and extruded to a length of 3657.6 mm to build a beam. Also, the different profiles were modeled in the beam and the hole was made in the beam to fit the cables inside the beam. The beam has two cables of 15.2 mm diameter for each profile and has two rebars of diameter 9.53 mm each in compression and tension side of the beam. The stirrup is of 4.53 mm diameter and placed at an equal distance of 114.3 mm each throughout the beam. The 3D model beam was now imported into the ANSYS geometry.

Element types and Meshing The engineering material used for the beam was selected to be concrete with a density of 2800kg/m³ and Young's modulus of 36050 Mpa. Also, structural steel was used for the rebar and the stirrup material and the structural steel material was edited with Young's modulus of 1.95*10⁵ Mpa for the pre-stress cable used. The connection between the concrete beam and stirrup was used as bonded. The no separation connection was assigned between the two pre-stress cables and the concrete beam.

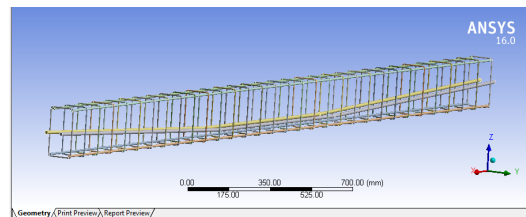


Figure 9: Modelling of cables, rebars and stirrups of beam

Tetrahedron method was used for the meshing with the meshing size of 25.4 mm for the beam model.

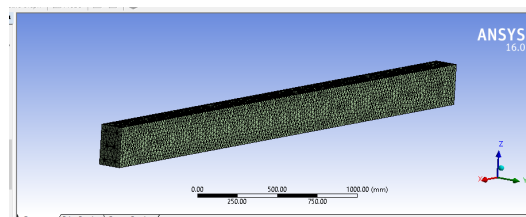


Figure 10: Meshing of the beam

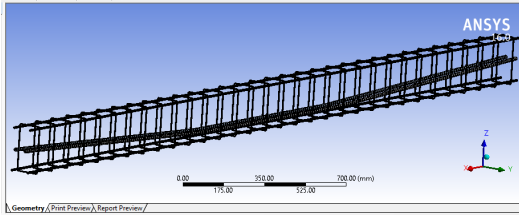


Figure 11: Meshing of the cable, rebar and stirrup

Boundary condition and loadings The boundary conditions were modeled as a simply supported beam. In the beam, one end had a fixed bottom edge while the other side was supported by rollers, so displacements at the x-axis were permitted. The one end faces of the cables at the roller support end were kept fixed and the pre-stress forces were applied at the other end faces of the cables. The directional deformation at the z-axis was inserted as the solution of the beam. The forces and the maximum directional deformation were set as parameters so that the changes in deformation can be calculated on the variation of the forces. The pre-stress forces on the cables were applied based on the static load test result of the cable. The breaking load for the 15.2 mm diameter cable was calculated to be 273 KN from the load test. The pre-stress forces were varied from 50% to 75% of the breaking load of the cable. Normally 75% of the breaking load is applied as the pre-stress force for the design of the post-tensioned beam. Figure 12 shows the analysis settings for the simulation of the beam in the ANSYS workbench.

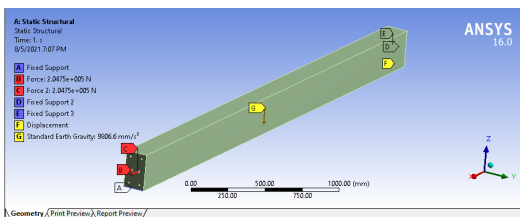


Figure 12: Boundary condition and loadings

3. Result and Comparison

3.1 Load test result

From the load test, it was found that the breaking load of 15.2 mm strand to be 273 KN. The phenomenon of breakage occurred at the gripping point of the anchorage and strand. The indentation of the grip or thread of the anchorage was seen on the strand. The ductile failure of a single outer ply occurred during the testing of the strand. The diameter of the inner ply was found to be 1.05 times greater than that of the

inner wire. The total area was calculated by adding the area of seven individual wires of the strand. The per meter weight of the strand was found to be 1127 g/m. Proof load at 1% extension was found to be 25100 kgf. The total area was calculated to be 143.19 mm² and from the stress vs strain graph, the modulus of elasticity of the strand was found to be 19554.44 kgf/mm².

Table 1: Physical properties of 15.2 mm strand

coilno.	6868/10	
laylength	203	mm
dia. of strand	15.38	mm
length	1.185	mm
weight	1336	gram
per mtr. weight	1127	gram/meter

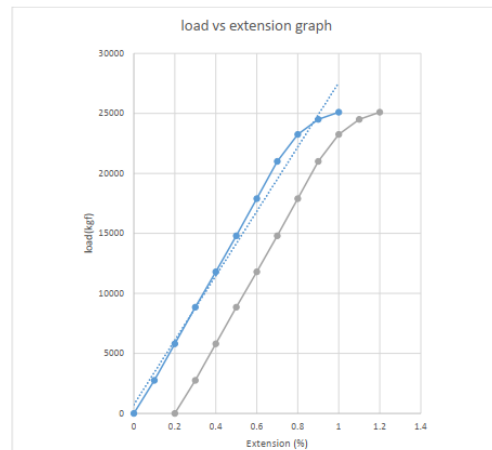


Figure 13: Stress VS Strain curve

Table 2: load test summary of 15.2 mm strand

Proof load(at 1% extension)	25100	kgf
Area	143.19	mm ²
Breaking Load	273	KN
Breaking Load	27800	kgf
MOE (load/area/ext.(0.1))	19554.44	kgf/mm ²

3.2 ANSYS model load test result

The simulation of the extension was also done in ANSYS. The 7-ply stranded wire was modeled in AutoCAD 3D and imported into ANSYS geometry where the properties of high tensile steel wire were given to the geometry and simulation for stress-strain analysis was done. The pre-stress force and the

deformation was set as a parameter to look at the changes due to the variation in those parameters.

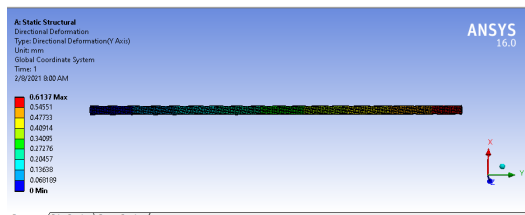


Figure 14: Directional Deformation of strand

Table 3: Variation of Direction Deformation on Magnitude of Directional Force

Directional Force (N)	Maximum Directional Deformation (mm)	Maximum Principle Stress (Mpa)
27000	0.6137	1373.4
57000	1.2956	2899.4
87000	1.9775	4425.4
115000	2.6139	5845.6
145000	3.2958	7375.6
176000	4.0004	8952.5
206000	4.6823	10478
228000	5.1824	11598
240000	5.4551	12208
246000	5.5915	12513
273000	6.2052	13886

3.3 Relaxation test result

For the 15.2 mm dia strand relaxation loss was calculated to be 1.16% i.e. the initial load of 18652 kgf was reduced to 18436 kgf at a load cycle of 100 hours. So the strand used in prestress process is also known as low relaxation high tensile strand due to its low relaxation loss over time and its high strength.

Table 4: Relaxation test report of 15.2 mm strand

Date	Time	Load	Relax.	(min)	(hr)
29-12-020	11:21	18652	0.0	0	0
30-12-020	7:21	18511	0.76	1200	20
31-12-020	03:21	18486	0.9	2400	40
31-12-020	23:21	18469	0.99	3600	60
01-01-020	19:21	18459	1.05	4800	80
02-01-020	15:21	18439	1.16	6000	100

3.4 Jacking and push in test

From the jacking test done at the site, similar properties of the cable were recorded. In a post-tensioning process done at the site, 75 % of the

breaking load is provided to the cable i.e. the cable is stressed at the load of 75 % of the breaking load for individual cable. The load is converted into pressure by dividing the force or load by the ram area of the jacking device and the efficiency of the jacking devices. No breakage of the cable was noticed at 75% load, after final stressing and locking force equal to 1.5 to 2 tons per strand was applied which resulted in the wedge set to 3 mm which is recorded as the anchorage slip or anchorage loss.

It was seen that if the three plies of the wedge of anchoring devices are not properly set and have a gap, it was noticed some amount of elongation of the strand was lost due to slipping of the strand due to improper sitting and gripping of the wedges.

Table 5: Wedge set loss

Force in cable(N)	Wedge set (mm)	Loss in Force (N)	Loss%
204750	3	22883.17	11.17

3.5 Mathematical results of deflection

During the analysis of post tensioned beam, concrete and cable is to be studied individually. The force in cable or pre stress force acts upward that gives the upward deflection on the beam whereas the self-weight and live load on the beam is acted downward. The equivalent uniformly distributed load, one point load and two equal point loads for parabolic, slopping and trapezoidal cable profile beam in equation (7), (10) and (15) is calculated. For Force in the cable is taken as 75% of the breaking load of the cable from load test.

$$\text{Force (F)} = 75\% \text{ of } 273 \text{ KN} = 204750 \text{ N}$$

$$\text{Maximum Eccentricity (a)} = e \text{ max} = 63.5\text{mm} \ \& \ 50 \text{ mm}$$

$$\text{Modulus of Elasticity for M40 grade of concrete is given by equation: } E = 5700\sqrt{fck} = 5700\sqrt{40}$$

$$E = 36050 \text{ Mpa}$$

$$\text{Section modulus (I)} = b*d^3/12 = 152.4*254^3/12$$

$$I = 208.12*10^6 \text{ mm}^4$$

$$\text{Length of beam (L)} = 3657.6 \text{ mm}$$

Table 6: Deflection results on different cable profile beam from mathematical model

Cable profile	Deflection for e= 63.5mm	Deflection for e= 50mm
Parabolic	4.83	3.80
Trapezoidal	4.75	3.74
Slopping	3.86	3.04

3.6 Stress on Beam

The direct stress at the end which is used to stress or tension the cable provides the compressive force on the beam results compressive stresses at the bottom and top fibre of the beam. The bending stress due to the eccentricity of the cable profile provides the compressive stress at the bottom fibre and tensile stress at the top fibre of the beam. The dead load and live load acted on the beam provides tensile stress at the bottom and compressive at the top fibre of the beam.

- Direct Stress

$$(\sigma_d) = P/A \quad (17)$$

Where, P is the pre-stressing force, A is end area.

$$P = 60\% \text{ of } 273\text{KN} = 177450 \text{ N}$$

$$(\sigma_d) = (2 * 177450)/(254 * 152.4) = 9.175\text{N/mm}^2$$

- Bending stress due to prestressing

$$(\sigma_p) = (M_p * y)/I = (P * e)/z \quad (18)$$

Where, Mp is Moment due to pre-stress, I is moment of inertia, e is the eccentricity, and z is section modulus of beam. $(\sigma_p) = (2 * 177450 * 63.5)/(152.4 * 254^2/6) = 13.75\text{N/mm}^2$

- Bending stress due to self weight

$$(\sigma_s) = (M_s * y)/I = (W_s * l^2)/(8 * z) \quad (19)$$

Where, Ms is Moment due to self weight, $(\sigma_s) = (0.93 * 3.6576^2)/(8 * 152.4 * 254^2/6) = 0.95\text{N/mm}^2$

- Bending stress due to live load

$$(\sigma_l) = (M_l * y)/I = (W_l * l)/(4 * z) \quad (20)$$

Where, Ml is Moment due to live load, $(\sigma_l) = (1.5 * 0.93 * 3.6576^2)/(8 * 152.4 * 254^2/6) = 1.42\text{N/mm}^2$

3.6.1 Resultant Stress

$$\text{Stress at top fibre } (\sigma_{top}) = \sigma_p - \sigma_d - \sigma_s - \sigma_l = 13.75 - 9.17 - 0.95 - 1.42 = 2.21\text{N/mm}^2$$

$$\text{Stress at bottom fibre } (\sigma_{bottom}) = -\sigma_p - \sigma_d + \sigma_s + \sigma_l = -9.17 - 13.75 + 0.95 + 1.42 = -20.55\text{N/mm}^2$$

3.7 Result from Finite Element Model

Using the methodology above mentioned in Finite element analysis, the deflection result was obtained from the simulation for different cable profiles and two different eccentricity.

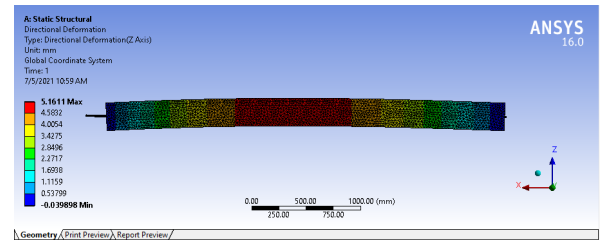


Figure 15: Deflection of Parabolic profile beam with e= 63.5 mm

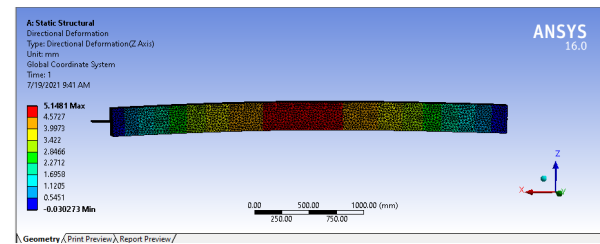


Figure 16: Deflection of Trapezoidal profile beam with e= 63.5 mm

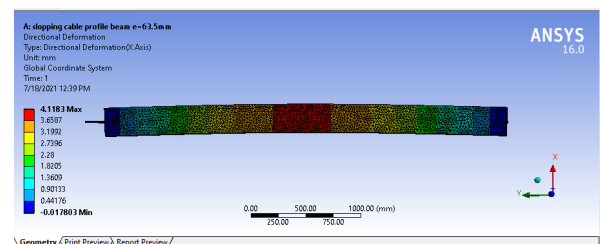


Figure 17: Deflection of Slopping profile beam with e= 63.5 mm

Table 7: Deflection results on different cable profile beam from ANSYS

Cable profile	Deflection for e= 63.5mm	Deflection for e= 50mm
Parabolic	5.16	4.08
Trapezoidal	5.14	4.07
Slopping	4.11	3.36

Stress result from Simulation From the simulation, the stresses at the top and the bottom of the beam is similar to that from numerical. The top part of the beam is subjected to the tensile stresses of 2.0145 KN/mm² and the bottom part is subjected to the compressive stresses of 20.937 KN/mm².

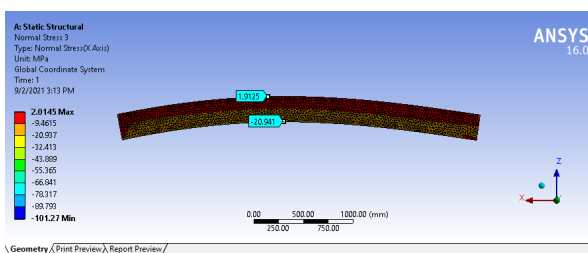


Figure 18: Stress in the beam

Pre stress Force VS Deflection result By setting the pre-stressing force and the maximum deflection as the parameters, it was easier to find out the maximum deflections by varying the pre-stressing force on the cable. The pre-stressing forces were varied from 50% to 75% of the breaking load of the cable i.e. 50%, 55%, 60%, 65%, 70% and 75% of 273 KN.

Table 8: Deflection of Parabolic profile beam due to variations in prestressing force

Force magnitude in cable 1 (N)	Force magnitude in cable 2 (N)	Maximum directional deformation (mm)
204750	204750	5.1611
191100	191100	4.8171
177450	177450	4.473
163800	163800	4.1289
150150	150150	3.7848
136500	136500	3.4408

Table 9: Deflection of Trapezoidal profile beam due to variations in prestressing force

Force magnitude in cable 1 (N)	Force magnitude in cable 2 (N)	Maximum directional deformation (mm)
204750	204750	5.1134
191100	191100	4.7725
177450	177450	4.4316
163800	163800	4.0907
150150	150150	3.7498
136500	136500	3.4089

Table 10: Deflection of Slopping profile beam due to variations in prestressing force

Force magnitude in cable 1 (N)	Force magnitude in cable 2 (N)	Maximum directional deformation (mm)
204750	204750	4.1183
191100	191100	3.8437
177450	177450	3.5692
163800	163800	3.2946
150150	150150	3.0201
136500	136500	2.7455

3.8 Modes of failure

The failure of pre-stress beam during the post-tensioning process occurs due to the following causes:

Cable failure During the post-tensioning process 75% force of the breaking load is provided to the cable in groups. The grouping of a number of cables is done according to the anchorage system used. The jacking force is converted into the modified pressure based on the ram area and efficiency of the jacking devices. The failure of the cable can be breakage or slippage which is caused due to following reasons:

- Rusted cable
- Rusted wedges and rusted wedge plate holes
- Worn teeth of wedges
- High friction points in ducts
- Overstressing



Figure 19: Breakage of Cable

A slip of a strand can occur during the stressing process or while anchoring the tendon. The slip of a strand can occur due to rusted wedges and rusted wedge plate holes. The rust or dirt will prevent the wedges from firmly gripping the strands. Worn teeth of jack wedge can be another reason for strand slipping. Strands slippage can be prevented by using well-maintained wedges, wedge plates, and jacks. Slippage of strands will be discovered from the marks made on strand's tails for this purpose. Slipped strands will have lower stress than other strands. This will reduce the overall force of the tendon. In order not to overstress other strands, the prestressing force should be reduced proportionally to account for the strand slip.



Figure 20: Slippage of Cable

Anchorage failure Anchorage is a set of devices that are used to tension the cable and lock the stressed cable. When the stressing process has been completed, anchorage transfers stressing pressure to concrete. The area that surrounds the anchorage devices where the stress concentration is high is known as the anchorage zone. This area is divided into two parts the local zone and the general zone. The size of the

local zone and the reinforcement used depends upon the anchorage system used. For the local zone, the main consideration is the presence of high compressive stresses and the need for confinement reinforcement to increase the concrete's compressive strength. The anchorage device comprises of anchor cone, anchor head and, wedges. Anchorage systems commonly used are Freyssinet, Magnel Blaton, Gifford-Udall, Leonhardt-Baur, LeeMCall, Dywidag, Roebling, and B.B.R.V.[6]. The anchor cone is fitted in the casting of the concrete, the anchor head has conical holes where the wedges sit to grip the cable. The main cause of the anchorage failure is the rusting of the wedges and rusting of the holes of the bearing plate. The rusted wedges are unable to grip the cable and slippage of the stressed cable occurs. The slippage of the cable results in the loss of prestressed force. Due to the higher hardness of the wedges the brittle failure of the wedges occurs during the locking of the stressed cable where the locking piston hammers the wedges by the locking plate.



Figure 21: Anchorage failure during Post-tensioning

The other mode of anchorage failure is the bursting of the anchor cone which is mainly due to the strength of the concrete, misalignment of the bursting reinforcement. Improper design and detailing of the anchorage zone can cause longitudinal and vertical cracks. The void and honeycomb in the end surface of the beam where the stress concentration is higher can lead to the failure of the post-tensioning process. During the post-tensioning process, the concrete beam is compressed, the eccentricity of the cable profile, the chambering of the beam occurs i.e the beam is deflected upward which leads to high compression at the bottom fiber of the beam and can cause the failure of the beam.



Figure 22: Beam failure during Post tensioning

Table 12: Deflection result comparison of beam with cable of eccentricity 50 mm

Profile with e= 50 mm	Deflection from mathematical model	Deflection from ANSYS	Diff. %
Parabolic	3.8	4.19	10.26%
Trapezoidal	3.74	4.07	8.82%
Slopping	3.04	3.36	10.53%

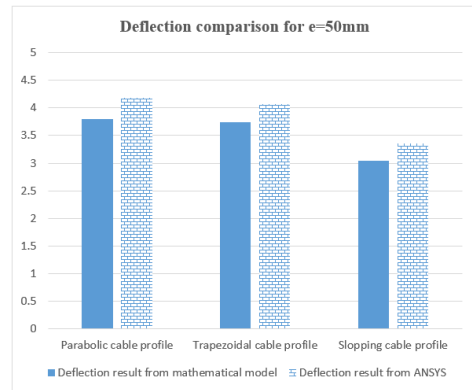


Figure 24: Comparison of deflection of beam with cable of eccentricity 50 mm

4. Comparison between mathematical and simulation result

Table 11: Deflection result comparison of beam with cable of eccentricity 63.5 mm

Profile with e= 63.5 mm	Deflection from mathematical model	Deflection from ANSYS	Diff. %
Parabolic	4.83	5.16	6.83%
Trapezoidal	4.75	5.14	8.21%
Slopping	3.86	4.11	6.47%

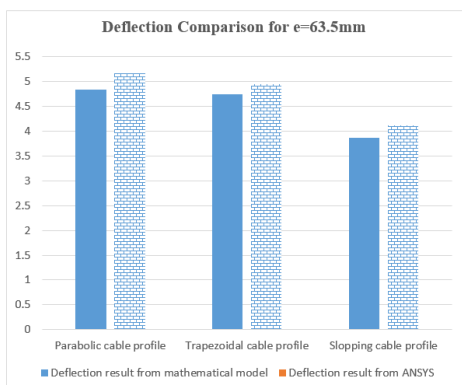


Figure 23: Comparison of deflection of beam with cable of eccentricity 63.5 mm

5. Conclusion

The study gives the experimental analysis on the cable anchorage system used in the post-tensioning process. The breaking load for the 15.2mm cable was recorded to be 273 KN and the breakage of the cable occurs at the gripping point of the wedges where one or more outer wire breaks first reducing the force which causes loss of prestressing force. The relaxation loss was recorded to be 1.16%. The wedge set also accounts for the loss in the prestressing force. For the wedge set value of 3mm, the percentage loss of prestressing force was calculated to be 11.17%. The rusting of the cable and wedges resulted in the slippage of the stressed cable. The losses during the post-tensioning process can be reduced by the use well-maintained cables, wedges, wedge plates, and jacks. The practice of threading the cable only before the tensioning of the cable can reduce rusting of the cable. The anti-rust coating of the cable and wedges can keep the cable and wedges fresh. The proper use of bursting reinforcement and higher strength of concrete without honeycomb and voids can reduce the chances of anchorage failure.

The parabolic profile gives maximum upward deflection for the same eccentricity and pre-stress

force. The maximum deflection of the beam occurred in the parabolic profile cables with an eccentricity of 63.5 mm and 50 mm was calculated to be 4.83 mm and 3.8 mm from the analytical method and was found to be 5.16 mm and 4.19 mm from simulation. The pre-stressing forces in the cables were applied on the based on the breaking load. Furthermore, higher eccentricity and higher prestressing force give higher upward deflection for the same profile of the beam. The deflection of the beam with an eccentricity of 63.5 mm for parabolic, trapezoidal and slopping cable profile beam was found to be 5.16 mm, 5.14 mm and 4.11 mm from simulation and 4.83 mm, 4.75 mm, and 3.86 mm from numerical simultaneously. The deflection results for three different cable profiles from both mathematical and simulation was compared and the difference is not more than 10.53%.

Acknowledgments

The authors are grateful to Dp wires, Wartex System, and Sai Manufacturing and Engineering for providing facilities and technical support and suggestions.

References

- [1] Haseeb Jamal. Advantages and limitations of prestressed concrete. *Structural Engineering*, 2017.
- [2] Aimee Corn. *Failure mode analysis of a post-tension anchored dam using linear finite element analysis*. PhD thesis, Colorado State University, 2014.
- [3] Kevin Q Walsh and Yahya C Kurama. Effects of loading conditions on the behavior of unbonded post-tensioning strand-anchorage systems. *PCI journal*, 57(1), 2012.
- [4] Ah Sir Cho and Thomas H-K Kang. Load-carrying performance and hydrostatic tests of encapsulated anchor systems for unbonded post-tensioning single-strands. *International Journal of Concrete Structures and Materials*, 12(1):1–10, 2018.
- [5] U Kim, PR Chakrabarti, and JH Choi. Nonlinear finite element analysis of unbonded post-tensioned concrete beams. In *Challenges, opportunities and solutions in structural engineering and construction*, pages 121–126. CRC Press, 2009.
- [6] Daniel A Abramson. *Comprehensive evaluation of multistrand post-tensioning anchorage systems for seismic resilient rocking wall structures*. University of Minnesota, 2013.